
Article:
Liu, X., Conte, M., Sankar, M. et al. (8 more authors) (2015) Liquid phase oxidation of cyclohexane using bimetallic Au-Pd/MgO catalysts. Applied Catalysis A: General, 504. pp. 373-380. ISSN 0926-860X

https://doi.org/10.1016/j.apcata.2015.02.034

Liquid phase oxidation of cyclohexane using bimetallic Au-Pd/MgO catalysts

Xi Liu [a], Marco Conte [a,b], Sankar Meenakshisundaram [a], Qian He [c], Damien M. Murphy [a], David Morgan [a], David Knight [a], Keith Whiston [d], Christopher J. Kiely [c] and Graham J. Hutchings [a, *]

[a] Cardiff Catalysis Institute, School of Chemistry, Cardiff University, Cardiff, CF10 3AT, UK

[b] Department of Chemistry, Dainton Building, University of Sheffield, Sheffield, S3 7HF, UK

[c] Department of Materials Science and Engineering, Lehigh University, 5 East Packer Avenue, Bethlehem, PA 18015-3195, USA

[d] INVISTA Textiles (UK) Limited, P.O. Box 2002, Wilton, Redcar, TS10 4XX, UK

*Corresponding author.

E-mail address: hutch@cardiff.ac.uk (G.J.Hutchings).

ABSTRACT: A detailed study of the selective oxidation of cyclohexane has been performed using bimetallic gold-palladium catalysts supported on magnesium oxide. Mono-metallic supported gold or palladium catalysts show limited activity for cyclohexane oxidation. However, a significantly enhanced catalytic performance is observed when supported gold-palladium alloy catalysts are used for this particular reaction. This synergy is observed for alloys spanning a wide range of gold-to-palladium molar ratios. Mechanistic studies reveal a promotion effect that occurs from alloying palladium with gold on the supported catalyst, which significantly improves the homo-cleavage of the O-O bond in cyclohexyl hydroperoxide, an important intermediate species in cyclohexane oxidation.

Keywords: gold catalysis. cyclohexane oxidation, EPR, STEM, oxidation.

1. Introduction

Aerobic oxidation of cyclohexane is of vital importance due to its use in nylon production [1]. In the present industrial production process, a facile aerobic alkane oxidation method is used, wherein materials such as cobalt naphthenate are utilised as an initiator to promote a radical autoxidation pathway [2,3]. Nevertheless, the autoxidation is not easily controlled, which means that the conversion must typically be kept below 5% in order to achieve > 80% selectivity to the desired alcohol and ketone products [4]. Unfortunately, the development of new efficient and green catalysts is significantly hindered due to kinetic inertness of both the alkane and O_2. Furthermore, a limited understanding of both the autoxidation and the catalytic oxidation routes exists in the literature as these reactions can be difficult to study. This often causes confusion and misinterpretation concerning the oxidation reaction which is complicated by autoxidation [5]. In order to develop new catalysts for this reaction that are capable of enhanced selectivity, more effective catalytic approaches and product analysis protocols are needed.

Gold catalysts are promising candidates for cyclohexane oxidation as they can activate molecular oxygen and enable oxidation under mild conditions [6-9]. However, a detailed study of the oxidation of cyclohexane by Hereijgers and Weckhuysen [10] pointed out inconsistencies in the literature concerning critical aspects of product analysis and mechanistic studies. They concluded that supported gold nanoparticles do not operate as a catalyst in the cyclohexane oxidation reaction, but rather as initiators which have a poor performance compared to the standard commercial cobalt naphthenate promoter [10]. On the other hand, we have recently shown that such behaviour can realistically be considered as falling somewhere in between these two extreme situations [11]. In fact, gold was found to be capable of accelerating the reaction, without the need for additional initiators, and so by definition could be considered to be a catalyst for the cyclohexane oxidation. However, the acceleration occurs by virtue of increasing the concentration of the intermediate species, which are chain carriers in the radical pathway of the reaction, and therefore promote catalytic autoxidation processes via a radical chain mechanism [11]. In addition, the enhancement in conversion caused by monometallic gold is limited when compared to autoxidation. This apparent dual nature of gold in cyclohexane oxidation prompted us to perform further studies in an attempt to achieve more efficient catalysts and gain deeper insights into both gold catalysis and catalytic aerobic oxidation when using gold-based alloy catalysts. In addition, a mechanistic study on promoted autoxidation is warranted due to the importance of this process in industrial nylon production, and could have a direct impact on other radical reactions, such as cobalt-mediated radical polymerization [12].

Previous studies have shown that the promising properties of Au can be manipulated by the addition of Pd to form Au-Pd bimetallic alloys as green catalysts [13-17]. Herein we report that Au-Pd nanoparticles supported on MgO can improve both conversion and product selectivity in the cyclohexane oxidation reaction as compared to the commercial cobalt naphthenate promoter. Furthermore, the improvements afforded by the MgO-supported Au-Pd particles are effective over a wide range of nominal Au:Pd compositions. Investigation of the reaction mechanism by means of electron paramagnetic resonance (EPR) and spin trapping experiments on the catalytic decomposition of cyclohexyl hydroperoxide (CHHP) are used to elucidate the origin of these beneficial effects.

2. Experimental

Chemicals. $HAuCl_4$, $PdCl_2$, cyclohexane and other chemicals were purchased from Aldrich and used without further purification unless otherwise specified.

Catalyst Preparation 1 wt% Au-Pd/MgO catalysts were prepared by using a modified sol-immobilisation method as reported previously [18]. The desired amount of $HAuCl_4$ and $PdCl_2$ were added to 800 mL water. After stirring for 15 min, 1.3 mL PVA solution (0.01 g/mL) was added and the solution was stirred for an additional 15 min. Subsequently, 3.295 mL freshly prepared $NaBH_4$ solution (0.1 M) was added to generate the Au-Pd nanoalloy particles. After reduction for 45 min, the MgO support (1.98 g) was added to immobilise the nanoparticles. After filtration and washing, the solid obtained was dried (110 ºC, 16 h) before use. The relative amount of gold and palladium salts used was varied in order to obtain a systematic series of supported catalysts with different molar ratios of Au-to-Pd, ranging from 20:1 to 1:20. Mono-metallic Au- or Pd- supported catalysts were also prepared for comparative purposes, using the same total metal loading (i.e. 1 wt%). Catalyst Testing. Catalytic oxidation of cyclohexane (Alfa Aesar, 8.5 g, HPLC grade) was carried out in a glass bench reactor using 6mg of catalyst. The reaction mixture was magnetically stirred at 140°C and 3 bar O_2 for 17 h. Samples of the reaction mixture were analysed by gas chromatography (Varian 3200) with a CP-Wax 42 column. Adipic acid was converted to its corresponding ester for quantification purposes, and chlorobenzene was added as an internal standard. Furthermore, $CBrCl_3$ (150 mg) was used as a carbon centred radical scavenger for studying the mechanisms in these oxidation reactions. $CBrCl_3$ was added into the reactor prior to the catalytic oxidation under identical reaction conditions. The product distribution as a function of reaction time was monitored by studying a systematic series of reaction batches subjected to different reaction times under the same conditions of temperature and oxygen partial pressure. Re-usability testing was also performed in an identical glass reactor. Cyclohexane (8.5g) and an additional amount of 1wt%Au-Pd/MgO (6mg) were added into the batch reaction and catalytic oxidation was carried out at 140°C and 3 bar O_2 for 17 h. After reaction, the 'used' catalyst was washed with cyclohexane and dried. Afterwards, the catalytic activity of the used Au-Pd/MgO catalyst was tested under the same reaction conditions (6 mg AuPd/MgO, 8.5 g cyclohexane, 140°C and 3 bar O_2 for 17 h). The obtained reaction mixture was analysed by gas chromatography[**19, 20, 21**]. Subsequent re-usability tests were carried out on the same material by following same procedure.

EPR Experiments. X-band continuous wave (CW) EPR spectra were recorded at room temperature in deoxygenated cyclohexane, using a Bruker EMX spectrometer. The typical instrument acquisition parameters were: centre field 3487 G, sweep width 100 G, sweep time 55 s, time constant 10 ms, power 5 mW, modulation frequency 100 kHz, and modulation width 1 G. Quantitative spectral analysis was carried out using WinSim software [22, 23]. The spin trapping experiments were performed using the following procedure: 5,5-dimethyl-1-pyrroline N-oxide (DMPO) (0.1 mL of 0.1 M solution in cyclohexane) was added to the substrate (0.1 mL of 2.5 molar % solution of CHHP in cyclohexane) in an EPR sampling tube. The mixture was deoxygenated by bubbling N_2 for 1 min prior to recording the EPR spectrum in order to enhance the signal [24]. For the reactions involving the Au/MgO, Pd/MgO and Au-Pd/MgO catalysts, de-oxygenation was carried out at room temperature 5 min after the mixing of the catalyst with the reaction mixture. Cyclohexyl hydroperoxide, was synthesized by a Grignard reagent-oxygen reaction [23, 25]. Finally, a solution of 2.5 mol% cyclohexyl hydroperoxide in cyclohexane was obtained.

Electron Microscopy Characterisation. Samples of catalysts were prepared for TEM/STEM analysis by dry dispersing the catalyst powder onto a holey carbon TEM grid. Bright field (BF) imaging experiments were carried out on JEOL 2000FX TEM operating at 200kV. High-angle annular dark field (HAADF) imaging experiments were carried out using a 200kV JEOL 2200FS scanning transmission electron microscope equipped with a CEOS aberration corrector. This latter microscope was also equipped with a Thermo-Noran X-ray energy dispersive spectroscopy (XEDS) system for compositional analysis.

3. Results and Discussion

3.1 Morphologies and catalytic performance of bimetallic catalysts.

Our initial studies were centreed on 1wt% Au-Pd/MgO catalysts prepared by sol-immobilisation. A representative bright-field (BF) electron micrograph of the as-prepared 1wt%Au-Pd/MgO material (with Au:Pd molar ratio of 1:1) is shown in Figure 1a. The mean size of the Au-Pd nanoparticles was found to be ca. 5.0 nm (Figure 1b). Aberration corrected STEM-HAADF imaging (Figure 1c) and XEDS analysis of individual particles (Figure 1d) in the bimetallic materials indicate that the supported particles are in fact homogenous Au-Pd random alloys. By comparison, the BF-TEM images of mono-metallic catalysts were also shown in Figure 1e and f. All three catalysts have very similar mean diameters of 5.0 nm (Au-Pd), 5.3 nm (Au) and 4.2 nm (Pd), respectively, confirming that particle size is unlikely to be the main reason for any measured differences in catalytic performance.

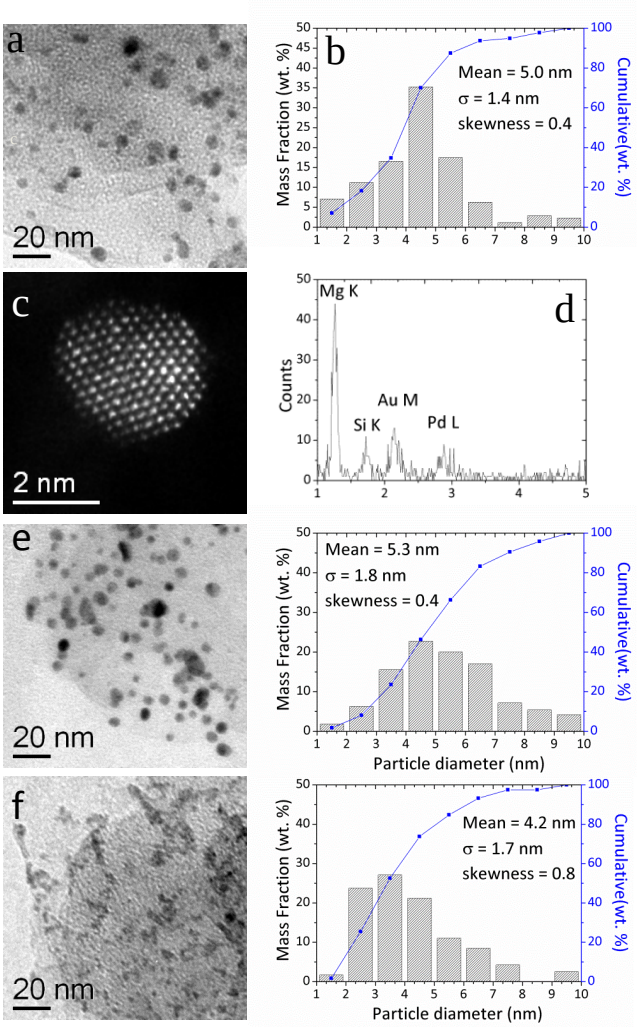

Figure 1. TEM images of various MgO supported metallic catalysts and their corresponding particle size distributions (PSDs). (a) Representative bright field TEM image of a 1wt% Au-Pd/MgO sol-immobilized catalyst; (b) particle size distribution (PSD) derived when sampling within the 1-10 nm size range; (c) representative HAADF-STEM image of an individual nanoparticle in the 1wt% Au-Pd/MgO catalyst; and (d) its corresponding XEDS spectrum, confirming that it is a Au-Pd alloy; e) BF image iof 1wt% Au/MgO (left) and corresponding particle size distributions (right): f) BF-TEM image of 1wt% Pd/MgO (left) and corresponding particle size distributions (PSDs) (right);

We investigated these catalysts for cyclohexane oxidation. 1wt%Au-Pd/MgO (Au: Pd molar ratio = 1:1) exhibited a conversion of 11% and a total selectivity of 95% which represents a potential improvement over the commercial cobalt naphthenate initiator (Table 1 and Figures 2a and 2b; for full by-product analysis and methodologies see supporting material, Figure S1 and S2, and Tables S1 and S2).By comparison, the monometallic Au/MgO and Pd/MgO counterparts display a much poorer catalytic performance, which confirms that neither Au nor Pd alone, act as an effective catalyst [9, 11, **26**]. Moreover, the supported Au-Pd catalyst displayed excellent stability, maintaining a 12% conversion and 98% selectivity even after being re-used multiple times (Table 2). We also tested the catalytic performance by means of GC [**19, 20, 21**] of a series of supported Au-Pd alloys having different nominal molar ratios (Figure 2b). It was found that the catalysts display a consistent catalytic performance over a wide spectrum of Au:Pd molar ratios (i.e. from 10:1 to 1:10). However, extremely Au-rich or Pd-rich catalysts are considerably less active, and tend towards the poorer performance exhibited by the two monometallic catalysts. The superior catalytic performance of 1wt%Au-Pd/MgO might be attributable to the modified exposed metal surface containing a mixture of Au and Pd atoms. As the enhanced activity is observed over a broad range of Au-Pd compositions, the precise Au:Pd ratio does not seem to be a crucial factor.

Table 1. Catalytic performance characteristics of cyclohexane oxidation over a variety of different catalyst materials ([a]).

Catalyst	Conversion (%)	Selectivity (%)				
		A	K	CHHP	AA	Total
1wt%AuPd/MgO	11	58	37	1	0	95
Co-naphthenate	9	45	37	0	2	85
$Fe(acac)_3$	7.7	35	48	0	0	82
Blank	1.1	22	19	57	0	98
MgO	1.0	40	35	20	0	95
1wt%Au/MgO	0.3	-	-	-	-	-
1wt%Pd/MgO	0	-	-	-	-	-

[a] Reaction conditions: 6 mg catalysts, 8.5 g cyclohexane, 140 °C, 3 bar O_2, 17 h; $Fe(acac)_3$ represents Fe(III) acetylacetonate. The acronyms A, K, CHHP and AA represent cyclohexanol, cyclohexanone, cyclohexyl hydroperoxide and adipic acid, respectively.

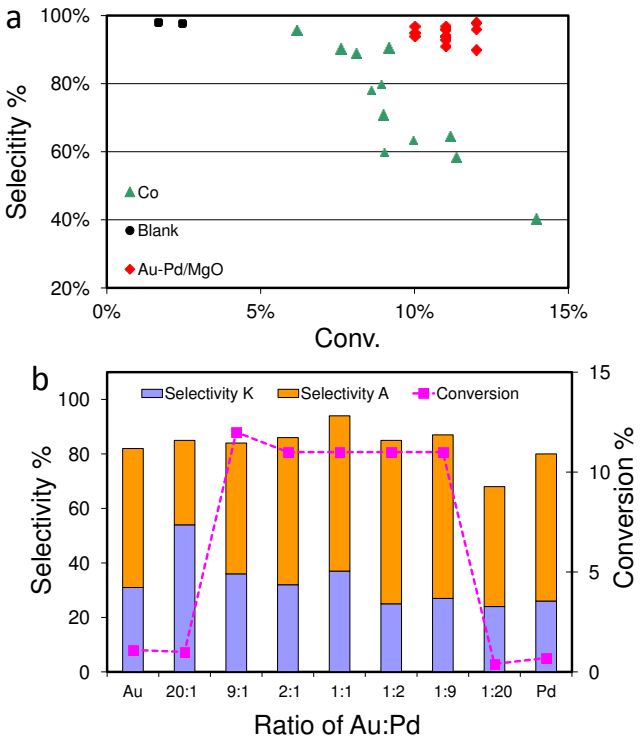

Figure 2. a) Comparison of various catalysts for cyclohexane oxidation, including a commercial Co promoted system (see supporting material, Table S2); b) Catalytic performance for cyclohexane oxidation using MgO supported Au-Pd as a function of the nominal Au:Pd molar ratio. The acronyms A, K and CHHP represent cyclohexanol, cyclohexanone, and cyclohexyl hydroperoxide respectively.

Table 2. Re-usability of the supported Au-Pd/MgO catalyst for cyclohexane oxidation.

Catalyst 1wt%AuPd/MgO	Conversion (%)	Selectivity (%)				
		A	K	CHHP	AA	Total
1st use	11	49	37	1	6	93
2nd use	11	49	37	1	6	93
3rd use	10	51	36	2	5	94
4th use	12	58	37	0	5	98

Reaction conditions: 6 mg catalyst, 8.5 g cyclohexane, 140 °C, 3 bar O_2, 17 h. The acronyms A, K, CHHP and AA represent cyclohexanol, cyclohexanone, cyclohexyl hydroperoxide and adipic acid, respectively. To test catalyst reusability, a reaction was conducted under the same reaction conditions but using a 120 mg batch of catalyst. After reaction the catalyst was collected and washed..Following this, 6 mg the used catalyst was tested for re-usability. A similar procedure was followed for subsequent re-cycle runs.

3.2 Mechanistic studies using EPR.

In our previous studies, we have used EPR to investigate the chemical nature of autocatalysis in cyclohexane oxidation [11]. EPR spectroscopy combined with the use of cyclohexyl hydroperoxide ($C_6H_{11}OOH$; CHHP) as a molecular probe has been used to definitively identify the different CHHP decomposition pathways. CHHP is a key intermediate in cyclohexane oxidation when the reaction is performed in the presence of noble metals or a cobalt salt [1]. This methodology offers a way to collect information on the the reaction mechanism of this reaction due to the large number or radical species involved [5]. In the current work, our EPR methodology has been extended, through both qualitative and quantitative studies of CHHP decomposition in the presence of cobalt naphthenate, Au/MgO, Pd/MgO and Au-Pd/MgO catalysts. (see Figure 3, and supporting information, Figures S3-S5).

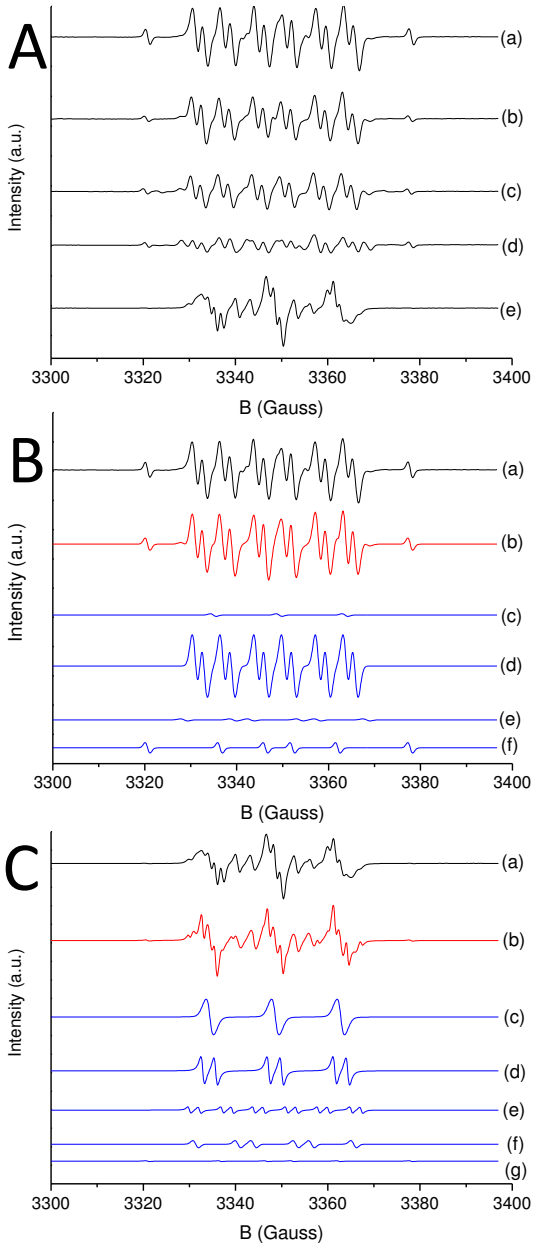

Figure 3 A EPR spectra of the DMPO spin adducts formed during the decomposition of CHHP in the presence of (a) Au-Pd/MgO, (b) Pd/MgO, (c) Au/MgO, (d) autoxidation and (e) Co-naphthenate (this final spectrum is reduced in scale by a factor of six in relation to the other plots);(.)

Figure 3B Deconvoluted EPR spectra of the 5,5-dimethyl-1-pyrroline N-oxide (DMPO) spin adducts obtained during the decomposition of CHHP in cyclohexane in the presence of 1wt% Au-Pd/MgO: (a) experimental spectrum and (b) simulated spectrum. Several species can be identified as follows- (c) A species with a_N = 14.31 G, which is a di-tertbutyl-nitroxide derivative, that can form by oxidation of DMPO) [**27**]; (d) a DMPO-O-C_6H_{11} spin adduct (a_N=13.37, $a_{H(\beta)}$ =6.01, $a_{H(\gamma)}$=1.90 G) [**e**]; (e) a DMPO-OO-C_6H_{11} adduct (a_N=14.49, a_H=10.64 G) [**29**]; and (f) carbon centered adduct (a_N=15.74, a_H=25.61 G), which is possibly a DMPO-C(OH)R_2 adduct [**30**] .

Figure 3C Deconvoluted EPR spectra of the 5,5-dimethyl-1-pyrroline N-oxide (DMPO) spin adducts obtained during the decomposition of CHHP in cyclohexane in the presence of Co-naphthenate: (a) experimental spectrum and (b) simulated spectrum. The species identified are as follows:- (c) a di-tertbutyl-nitroxide derivative (a_N = 14.18 G) [**31**]; (d) an unidentified nitroxide from DMPO with coupling constant a_N = 14.30, a_H = 2.81 G that could arise from decomposition of the spin trapping molecule [**32**]: (e) a DMPO-O-C_6H_{11} spin adduct (a_N=13.97, $a_{H(\beta)}$=7.01, $a_{H(\gamma)}$=2.2 G); (f) a DMPO-OOR/OOH adduct (a_N=12.54, a_H=9.15 G) and (g) a carbon centred adduct (a_N=15.67, a_H=25.67 G),which is possibly a DMPO-C(OH)R_2 adduct [**30**].

Simulation of the EPR spectrum and comparison with literature values allows us to identify all the radical intermediates which were anticipated to be present in the autoxidation of cyclohexane to cyclohexanone and cyclohexanol; namely: a di-tert butyl-nitroxide derivative (a_N = 14.2G); a DMPO-O-C_6H_{11} spin adduct (a_N=13.4, $a_{H(\beta)}$=6.01, $a_{H(\gamma)}$=1.80G); a DMPO-OOC_6H_{11} adduct (a_N=14.2, a_H=10.9G); and a DMPO-C carbon centred adduct, possibly of a carbon hydroxylated species (a_N=15.8, a_H=25.7G) that could account for adipic acid (Figure 3 and supporting information, Figures. S3-S5) [**33**]. We note a significant difference between CHHP decomposition in the presence of Au-Pd and Co naphthenate in Figure 3. The relative concentration of the species found in presence of Au-Pd are: di-tertbutyl-nitroxide derivative: 3.7%; DMPO-O-C_6H_{11}: 87.8%; DMPO-OOH/R adduct: 2.9%; and a possible DMPO-C(OH)R_2 adduct: 5.6%. However, the relative concentration of the species generated when using the Co salt are: di-tertbutyl-nitroxide derivative: 44.4%; nitroxide from DMPO decomposition by peroxides: 36.4%; DMPO-O-C_6H_{11}: 8.3%; DMPO-OOH/R adduct: 8.9%; and a possible DMPO-C(OH)R_2 adduct: 2%. This analysis confirms that the role of Au-Pd is different from the commercial promoter in this reaction. However, It should be stressed that the spin trapping technique only allows for semi-quantitative determination of the spin adducts detected, and it is

not a direct measurement of the actual amount of radical species present in solution. Therefore it is not possible to quantitatively correlate reactivity, or lifetime, of a radical to its correspondent spin adduct, but qualitatively only This is a consequence of various factors such as: the life-time of the spin adduct, the nature of the solvent, temperature, pH and importantly, the efficiency of the capture reaction which is different for each radical [**35**,**36**]. For example, literature values comparing the capture of ·OOH versus ·OH species for DMPO in aqueous media at room temepruare and pH close to neutrality indicated kinetics constants in the range of 10^1 and 10^9 M s^{-1} for ·OOH and ·OH respectively [**37**]. Therefore, the detection of spin adducts of similar intensity for these species actually means that the concentration of peroxides is of some order of magnitude higher than the concentration of hydroxyl species. Moreover, when heterogeneous catalysts are used, spin trapping molecules may also be capable to abstract species weakly bound over the catalyst surface **[38]**. With these limitations in mind, the deconvoluted spectra simulations led to the values reported in Table 3 for the various catalysts used.

The species trapped in the presence and absence of Au/MgO, Pd/MgO and Au-Pd/MgO catalysts are basically the same in all sets of experiments, with the exception of the detection of the carbon parent radical (spin adduct: C_6H_{11}-DMPO) when Au/MgO was used (ca. 3% amount of DMPO spin adduct). However, the most remarkable difference noted between these data sets is the increased amount of DMPO-alkoxyl (C_6H_{11}-O-DMPO) species versus DMPO-peroxyl (C_6H_{11}-OO-DMPO) species from ca. 2 to > 10 when Au or Pd containing materials are used compared to the pure autoxidation or blank test materials. This indicates that the MgO supported metal catalysts are capable of homo-cleavage of the O-O bond in CHHP.

Moreover, the co-existence of Au and Pd in the form of an alloy significantly promotes the O-O bond dissociation, wherein the ratio of alkoxyl species to peroxyl DMPO spin adduct species doubles compared to that of monometallic Auor Pd(Table 3). It should be further stressed that because also of the kinetics of the spin trapping reaction, these are relative changes. However, considering the kinetics of the capture reaction the be the same because the reaction media is the same, regardless the metal promoters used, we consider our reasoning still valid. This suggests that the Au-Pd alloy has an intrinsically stronger chemical affinity for cyclohexyl hydroperoxide, resulting in homo-cleavage of the O-O bond. In order to explain this effect, the electronic structure at the surface of Au-Pd nanoparticles needs to be considered. In fact, both Au and Pd are capable of enhancing the formation of alkoxide intermediates, when compared to autoxidation, although it is only the MgO supported Au-Pd alloy that displays an enhanced conversion, i.e. a higher turnover frequency. Unlike the monometallic case, if Au and Pd are alloyed, a shift of electron density from Pd to Au atoms can occur [14, 39], while preserving a higher electronegativity on the Au [40]. (i.e. in case of the simultaneous presence of Au and Pd, Au is the more electronegative). Hence, the adsorption of CHHP over an active site comprising neighbouring Au and Pd atoms will more favourably lead to the cleavage of the O-O bond in CHHP due to the difference in induced charge between the two metal components, which exist as a $Au^{\delta-}$-$Pd^{\delta+}$ couple (Scheme **1**) and this we consider gives an electronic basis for the origin of the synergistic effect that is clearly observed when Pd is added to Au (and vice versa) for this, and possibly other, redox reactions. This enhancement can be observed for a broad range of Au:Pd compositions, rather than a narrow composition where synergy has been observed in previous studies for other redox reactions [15-17]; but clearly requires a minimum level of either metal since compositions with either low amounts of Au or Pd are ineffective in the bimetallic catalysts.

Table 3. Quantification and characterization of the DMPO spin adducts from EPR spin trapping experiments.

Catalyst	Nitroxide	RO·	ROO·	Carbon radicals	RO·/ ROO· ([a])
Autoxidation	2.3	63.2	29.6	4.9	2.1
1wt%Au/MgO	5.9	82.5	5.3	6.3	15.6
1wt%Pd/MgO	5.5	82.1	6.4	6.0	12.8
1wt%AuPd/MgO	3.7	87.8	2.9	5.6	30.3
Co-naphtenate	44.4(36.4)c	8.3	8.9	2.0	0.9

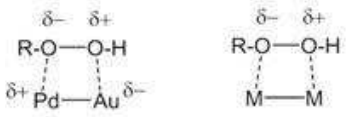

Scheme 1: Specific surface substrate adsorption of CHHP in the case of a bimetallic Au-Pd catalyst (left) and non-specific surface substrate adsorption of CHHP in case of a monometallic catalyst (right). As a consequence, a promoted, or in our case catalytic, decomposition of CHHP occurs (see eq. 1) thus favouring alkoxide formation at a faster rate, and in turn a higher level of conversion.

C_6H_{11}-OOH → C_6H_{11}-O· + ·OH (eqn.1)

A similar decomposition route operates in manganese aluminophosphate catalysts, where CHHP decomposes by adsorption on a $Mn^{\delta+}$-$O^{\delta-}$ moiety [41]. Despite the obvious differences between a metal nanoparticle and an aluminophosphate surface, for the latter system it was proposed that an orienting effect on the CHHP molecule was induced by the dipolar nature of the Mn and O neighbours. We postulate that an analogous effect can take place in the case of Au-Pd bimetallic nanoparticles. In fact, for the case of monometallic Au or Pd where an active site such as Au-Au or Pd-Pd will be present, the cleavage solely results from the adsorption of the hydroperoxide, but without any specific orientation of the substrate. By way of direct comparison, cobalt-initiated autoxidation predominantly produces peroxide species, including cyclohexyl peroxide and derivative nitroxide radicals, whereas the amount of alkoxy radicals generated is only 8.3%. This is evident from figure 3-C, spectra (c) and (d), which are indicative of a peroxide amount in solution that is so high that it causes degradation of the spin probe [**32**]. Even so, the fraction of the peroxy radicals detected in case of Co naphthenate is still significantly higher than in the presence of the supported Au-Pd catalyst. The strong production of peroxide species was attributed to the cobalt species favouring the attack of CHHP and the generation of ROO· in agreement by the Haber-Weiss cycle.[**42,43**]. Which is preceded by cyclohexyloxyl radical formation. It should also be considered that peroxide species ROO· are known to be less reactive than RO· radicals [**32,34**] which could lead to a slower reaction rate and lower conversion. A usually accepted Haver-Weiss cycle and termination reaction of the alkyl peroxide intermediate is reported below[**42,43**]:

R-OOH + Co^{II} → Co^{III}-OH + RO· (eqn. 2)

Co^{III}-OH + R-OOH → Co^{II} + ROO· + H_2O (eqn. 3)

with the nett resulting equation:

2C_6H_{11}-OOH → C_6H_{11}-OO· + C_6H_{11}-O· + H_2O (eqn. 4)

Disproportionation [2, 3]

2C_6H_{11}-OO· → C_6H_{11}-OH + C_6H_{10}=O + O_2 (eqn. 5)

As a consequence of this set of reactions, a commonly used way to estimate radical species lifetime, which would affect both: the amount of spin adducts detected and the efficiency of the oxidation reaction, is to use the equation:[**44**]

$$\tau_c = \frac{1}{2k_{term}[X\cdot]_s}$$

where k_t is the average termination kinetic parameter and $[X\cdot]_s$ is the steady-state radical concentration. This well apply to polymerizarion reaction, however, by definition it also assumes a steady state radical concentration, in this case the chain carrier (wich in our case would be ROO·) and the prodcuts formation at the termination step[**45**] (which in our case would be eq. 5). On the other hand, recent studies by Hermans and co-workers showed that a more accurate pcitures of the cyclocheance oxidation should not be limited to steady state considitons, but rather the use of quasi-steady state concetrations[**46**]. which in our cae and for ROO· would lead to:

$$[C_6H_{11}OO\cdot]_{qss} = \sqrt{\frac{k_{init}[C_6H_{11}OOH]}{k_{term}}}$$

Where k_{init} and k_{term} are the rate constants of the initiation and termination reaction respectively. This is more complex than a classical scheme based on termination only and on the final [ROO·] concentration. In fact, whereas the termination step proceed with a very low activation barrier [2] and a pure association of two radical species, the term k_{term} is unlikely to be affected by significant traces of additives/metals. In contrast, the initiation reaction has a high activation energy (usually estimated in the range of ca. 170 kj/mol) [**47**] therefore Even a relatively small decrease of the effective barrier, operated in our case by different metals, should therefore lead to a substantial increase in $[C_6H_{11}OO\cdot]$qss and hence to an increase in the hydrocarbon (R-H) oxidation rate [**46**]. This has obvious consequences on: effective radical lifetime and in turn the species actually trapped by DMPO and importantly the catalytic nature of the oxidation reaction (vide infra), with quantitative effects that are difficult to predict a priori.

In fact, as a consequence of these usually accepted reaction schemes, this suggests that both alkoxyl and peroxyl radicals are primary products of the Co-promoted decomposition of CHHP, (and this either the Haber Weiss cyle takes palce via a pure radical pathway [**42,43**] or involving H+ or OH- species [**48**]) And once the peroxide radical has formed, disproportionation (eq. 5) would follow and initiate the autoxidation process again (eqns. 6-9). However, our work shows that for MgO supported Au-Pd nanoparticles present a much higher amount (in relative terms) of alkoxyl adducts rather than peroxyl adducts. This is evident from Figure 3-B where the spectrum is entirely dominated by alkoxide species (spectrum d) andwhich would suggest a dominance of eq. 6.

Initiated autoxidation:

$C_6H_{11}\text{-}O\cdot + C_6H_{12} \rightarrow C_6H_{11}\cdot + C_6H_{11}\text{-}OH$ (eqn. 6)

However for completeness we consider important to describe other sptes that are involved in the autoxiation process and that could help to clarify differences and similarities between Co and AuPd systems, as well as pure autoxidation. In fact once the $C_6H_{11}\cdot$ radical is formed (eiter at the initiation stetp or from eq. 6) this will immeditately react under diffusion control [**49**] with any oxygen present in solution.

$C_6H_{11}\cdot + O_2 \rightarrow C_6H_{11}\text{-}OO\cdot$ (eqn. 7)

On the other hand, pure radical combinations are not the only pathways that operatives in these reaction and of particular importance are eq 8 and eqn 9 below [**2, 46**]

$C_6H_{11}\text{-}OO\cdot + C_6H_{11}\text{-}OOH \rightarrow C_6H_{11}\text{-}OOH + C_6H_{10}(\cdot)OOH$ (eqn. 8)

$C_6H_{10}(\cdot)OOH \rightarrow C_6H_{10}{=}O + \cdot OH$ (eqn. 9)

In this case, cobalt does not have any further direct contribution to the subsequent autoxidation after it has reacted with peroxide (eq. 1). Of particular importance is eq. 8, in fact, recent studies[**50**] shows that these reactions take place by means of solvent cage and once the product from abstraction of a H in α is obtained (C6H10(·)OOH) the ketone is obtained (eq. 9) without the need of a 'standard' termination step (eq. 4). This will necessarily need to the ketone as product an without the need of any additioan metal species in solution.

On the other hand Au-Pd bimetallic catalysts are capable of an enhanced selectivity to cyclohexanol compared to Co and Fe thus suggesting an enhanced cleavage of the O-O bond of CHHP.. Consequently, even in the autoxidation, the supported metallic catalysts still participate in the selective decomposition of CHHP (see Scheme 1), and lead to improvements in overall conversion and selectivity, minimizing uncontrollable ring-opening reactions, which would lead to the production of acids and esters [**48,50**]. (.)

To further prove this important aspect, we have also used a carbon-centred radical scavenger, $CBrCl_3$, to quench the autoxidation pathway, in order to differentiate the autoxidation process from the catalytic oxidation [**11**] As $CBrCl_3$ can quench carbon centred radicals by means of bromo-hydrocarbon formation.[**51**] It should be noted that the use of dialkyl nitroxides for the capture of carbon cantered radicals has been avoided for this particular reaction. This because reaction conditions (solvent free and reaction temperature of ca. 140 ^{o}C), and the presence of metal centres can trig hydrogen abstraction reactions[**52**] as well as oxidation of the alcohol to the ketone,[**53**] and we wanted to minimize the presence of parallel and undesired reaction pathways.

When an excess amount of $CBrCl_3$ (150 mg) was added, no oxidation of cyclohexane was observed in the presence of cobalt naphthenate, which confirms that the cobalt salt acts as promoter rather than a catalyst. By way of comparison, with the Au-Pd/MgO material, both oxygenation and bromination of cyclohexane took place from the very beginning of the reaction in the presence of $CBrCl_3$ (Figure 4), which demonstrates that the supported Au-Pd particles have a strong resistance to this radical scavenger, which would suggest a different oxidation pathway with an enhanced CHHP decomposition compared to Co.

(.)In any case, we consider that any new reaction pathways induced by AuPd is not involving a direct O_2 activation/adsorption. In fact, once the C_6H_{11}· radical is formed, this would react with O_2 under diffusion controlled conditions [**54,55**], and the C_6H_{11}-OO· radical or C_6H_{11}-OOH species will only adsorb to the catalyst surface afterwards. This diminishes the possibility of oxidation occurring via an η_2 oxygen intermediate (i.e. with both oxygen atoms of molecular oxygen adsorbed over the catalyst surface), as it would involve a switch in the oxidation state of the metal [**56**]. Furthermore this process would be slower than for a diffusion controlled route where O_2 reacts directly with the C_6H_{11}· radical [18].

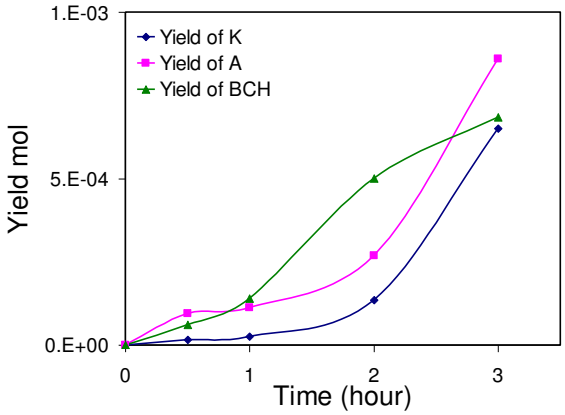

Figure 4. Formation of various products as a function of reaction time in the presence of $CBrCl_3$ when using the Au-Pd/MgO catalyst. Key to the shorthand notation used:- A, K, and BCH represent cyclohexanol, cyclohexanone, and bromocyclohexane respectively.

Oxygen, could still in principle play a role if hydride intermediates are present, as in the case of β-elimination of alcohols [22] since it would be involved in the regeneration of the active metal site, via formation of non-alkyl hydroperoxide intermediates. However, the spin trapping experiments do not show any evidence of pure hydroperoxide intermediates, only alkyl peroxide species, thus supporting the notion of adsorption of ROO· or ROOH substrates onto the catalyst surface.

Nevertheless, the enhanced CHHP decomposition still lead to species that are detected also in presence of Co (ROO· and RO·) and therefore this is still an autoxidation pathway. However, our data would suggest that while Co operates a promotion to autoxidation by means of peroxyl species, AuPd would operate by enhancing the amount of alkoxyl species.

3. Conclusions

For the selective oxidation of cyclohexane, we consider that it is possible to classify the supported Au-Pd material both as a catalyst, as well as an initiator, since the bimetallic material remains persistently active during the whole oxidation process for peroxide decomposition.. The presence of Au-Pd nanoparticles clearly has a significant positive influence on the overall catalytic performance in cyclohexane oxidation, and in particular, inhibits production of unwanted by-products. We show that the free radical chain pathway can be manipulated by selectively decomposing the peroxide intermediate to improve the overall catalytic performance and productivity. Our data suggest a cooperative effect between Au and Pd that could induce an orienting effect of the CHHP intermediate moiety..

Acknowledgements

The authors wish to acknowledge the support of INVISTA Textiles (UK) Limited, INVISTA Intermediates and INVISTA Technologies S. à r. l. C.J.K gratefully acknowledges funding from the National Science Foundation Major Research Instrumentation Program (GR# MRI/DMR-1040229).

References

[1] U. Schuchardt, D. Cardoso, R. Sercheli, R. Pereira, R. S. da Cruz, M. C. Guerreiro, D. Mandelli, E. V. Spinacé, E. L. Pires, Appl.Catal. A: Gen. **211** (2001) 1-17.

[2] I. Hermans, T. L. Nguyen, P. A. Jacobs, J. Peeters, Chem.Phys.Chem **6** (2005) 637-645.

[3] I. Hermans, P. A. Jacobs, J. Peeters, Chem. Eur. J. **12** (2006) 4229-4240.

[4] U. Schuchardt, W. Al. Carvalho, E. V. Spinacé, Synlett. **10** (1993) 713-718.

[5] J. Kim, R. G. Harrison, C. Kim, L. Que, J. Am. Chem. Soc. **118** (1996) 4373-4379.

[6] T. Ishida, M. Haruta, Angew. Chem. Int. Ed. **46** (2007) 7154-7156.

[7] Y. J. Xu, P. Landon, D. Enache, A. F. Carley, M. W. Roberts, G. J. Hutchings, Catal. Lett. **101** (2005) 175-179.

[8] G. Lu, R. Zhao, G. Qian, Y. Qi, X. Wang, J. Suo, Catal. Lett. **97** (2004) 115.

[9] L. X. Xu, C. H. He, M. Q. Zhu, S. Fang, Catal. Lett. **114** (2007) 202-205.

[10] B. P. C. Hereijgers, B. M. Weckhuysen, J. Catal. **270** (2010) 16-25.

[11] M. Conte, X. Liu, D.M. Murphy, K. Whiston, G.J. Hutchings, Phys. Chem. Chem. Phys. **47** (2012) 16279- 16285.

[12] R. K. Biyani, R. V. Subramanian, R. Mahalingam, J. Appl. Pol. Sci. **25** (1980) 1257-1260.

[13] J. K. Edwards, G. J. Hutchings, Angew. Chem. Int. Ed. **47** (2008) 9192-9198.

[14] J. Pritchard, L. Kesavan, M. Piccinini, Q. He, R. Tiruvalam, N. Dimitratos, J.-A. Lopez-Sanchez, A. F. Carley, J. K. Edwards, C.J. Kiely, G. J. Hutchings, Langmuir **26** (2010) 16568-16577.

[15] R. Su, L. Kesavan, M.M. Jensen, R. Tiruvalam, Q. He, N. Dimitratos, S. Wendt, M. Glasius, C. J. Kiely, G. J. Hutchings, F. Besenbacher, Chem. Commun., In Press (2014) DOI: 10.1039/C4CC04024D

[16] G. J. Hutchings, Catal. Today, In Press (2014) DOI: 10.1016/j.cattod.2014.01.033

[17] E. Nowicka, J. P. Hofmann, S. F. Parker, M. Sankar, G. M. Lari, S. A. Kondrat, D. W. Knight, D. Bethell, B. M. Weckhuysen, G. J. Hutchings, Phys. Chem. Chem. Phys., **15** (2013) 12147-12155

[18] B. A. Steinhoff, S. S. Stahl, Org. Lett. **4** (2002) 4179-4181.

[19] L. Zhou, J. Xu, H. Miao, F. Wang, X. Li, Appl. Catal. A: Gen. 292 (2005) 223–228.

[20] S.B. Turnipseed, A.J. Allentoff, J.A. Thompson, Anal. Biochem. **213** (1993) 218–225.

[21] R. Raja, P. Ratnasamy, Catal. Lett. **48** (1997), 1–10.

[22] Simulations were carried out using WinSim software: http://www.niehs.nih.gov/research/resources/software/tox-pharm/tools/index.cfm.

[23] M. Conte, K. Wilson, V. Chechik, Org. Biomol. Chem. **7** (2009) 1361-1367.

[24] C. Walling, S. A. Buckler, J. Am. Chem. Soc. **77** (1955) 6032-6038.

[25] G. J. Hutchings, Dalton Trans. (2008) 5523-5536.

[26] J. Long, H. Liu, S. Wu, S. Liao, Y. Li, ACS Catal. **3** (2013) 647-654.

[27] E. G. Janzen, B. J. Blackburn, J. Am. Chem. Soc. **91** (1969) 4481-4490

[28] S. L. Baum, I. G. M. Anderson, R. R. Baker, D. M. Murphy, C. C. Rowlands, Anal. Chim. Acta. **481** (2003) 1-13.

[29] M. J. Davies T. F. Slater, Biochem. J. **240** (1986) 789-795.

[30] E. G. Janzen, J.-P. Liu, J. Magn. Reson. **9** (1973) 510-512.

[31] M. Conte, H. Miyamura, S. Kobayashi, V. Chechik, Chem. Commun. **45** (2010) 145-147.

[32] M. Conte, K. Wilson, V. Chechik, Rev. Sci. Instrum. **81** (2010) 104102-104108.

[33] E. J. Silke, W. J. Pitz, C. K. Westbrook, M. Ribaucour, J. Phys. Chem. A **111**, 2007, 3761–3775.

[34] M. Conte, V. Chechik, Chem. Commun. **46** (2010) 3991-3993.

[35] P. Ionita, M. Conte, B. C. Gilbert, V. Chechik, Org. Biomol. Chem. **5** (2007) 3504-3509.

[3136] P. Ionita, B. C. Gilbert, A. C. Whitwood, Perkin Trans. **2** (2000) 2436-2440.

[37] E. Finkelstein, G. M. Rosen, E. J. Rauckman, J. Am. Chem. Soc. 102 (1980) 4994–4999.

[**38**] M. Conte, H. Miyamura, S. Kobayashi, V. Chechik, J. Am. Chem. Soc. 131 (2009) 7189–7196 9.

[39] Z. Li, F. Gao, Y. Wang, F. Calaza,L. Burkholder, W. T. Tysoe, Surf. Sci. **601** (2007) 1898-1908.

[40] M. Conte, A. F. Carley, G. Attard, A. A. Herzing, C. J. Kiely, G. J. Hutchings, J. Catal. **257** (2008) 190-198.

[41] B. Modén, B.-Z. Zhan, J. Dakka, J. G. Santiesteban, E. Iglesia, J. Catal. **239** (2006) 390-401.

[42] J. Weinstein, B. H. J. Bielski, J. Am. Chem. Soc. 101 (1979) 58–62.

[43] S. Tanase, E. Bouwman, J. Reedijk, Appl. Catal. A: Gen. 259 (2004) 101–107.

[**44**] S. K. Reddy, N. B. Cramer, Christopher N. Bowman, Macromolecules 39 (2006) 3673–3680.

[**45**] G. Odian, Principles of Polymerization, 3rd ed.; John Wiley & Sons: New York, (1991).

[**46**] I. Hermans, J. Peeters, P. A. Jacobs, ChemPhysChem. 7 (2006) 1142–1148.

[**47**] C. A. Tolman, J. D. Druliner, M. J. Nappa, N. Herron, in: Activation and Functionalization of Alkanes (Ed.: C. L. Hill), Wiley, New York, (1989).

[48] B. P. C. Hereijgers, B. M. Weckhuysen, J. Catal. 270 (2010) 16–25.

[49] M. S. Stark, J. Am. Chem. Soc. 122 (2000) 4162-4170.

[**50**] I. Hermans, P. Jacobs, J. Peeters, Chem. Eur. J. 13 (2007) 754 – 761.

[**51**] S. V. Dvinskikh, A. V. Yurkovskaya, H.-M. Vieth, J. Phys. Chem. 100 (1996) 8125–8130.

[**52**] C. Berti, M. J. Perkins, J. Chem. Soc. Chem. Comm. (1979) 1167-1168.

[**53**] A. Dhakshinamoorthy, M. Alvaro, Hermenegildo García, ACS Catal. 1 (2011) 48–53.

[54] N. A. Porter, J. Org. Chem. **78** (2013) 3511-3524.

[55] J. M. Keith, W. A. Goddard III, Organometallics **31** (2012) 545-552.

[56] F. Acke, I. Panas, J. Phys. Chem. B **102** (1998) 5158-5164.

Received: ((will be filled in by the editorial staff))
Revised: ((will be filled in by the editorial staff))
Published online: ((will be filled in by the editorial staff))

Highlights

• Unique catalytic performance of Au-Pd bimetallic catalysts on MgO for cyclohexane oxidation

• Identification of evolution of an intermediate by using EPR

• Evident difference between Co catalyst and Au-Pd nano alloy

• Pd modified by alloying with Au has a higher activity for O-O catalytic dissociation.

Graphical abstract